



## Structural, optical and antibacterial studies of pure and amino acid added sulphamic acid crystals

Fredselin R.S Vithel<sup>1</sup> and R. Manimekalai<sup>2\*</sup>

<sup>1</sup> Research scholar, Department of Physics, A.V.V.M Sripushpam College, Poondi, Thanjavur, Affiliated to Bharathidasan University, Tamil Nadu, India.

<sup>2</sup> PG and Research Department of Physics, A.V.V.M Sripushpam College, Poondi, Affiliated to Bharathidasan University, Tamil Nadu, India

\*Corresponding Author: maniabi64@gmail.com

---

### Abstract

The pure sulphamic acid (SA) and some amino acids added sulphamic acid crystals were grown successfully by slow evaporation technique at room temperature. The structural studies revealed that both SA and amino acids added SA crystals possessed orthorhombic crystal structure. The presence of vibrational modes and existence of carbon in the system was also confirmed using FTIR analysis. The surface morphology of crystals was studied. The optical transparency and band gap of the grown crystals were calculated. The hardness of amino acid added crystal is relatively higher than that of the pure SA crystals. The thermal stability of the grown crystals was analyzed by thermo gravimetric and differential thermal analysis (TGA/DTA), which revealed that the grown crystals were thermally stable and elevated from 261°C to 278°C for amino acid added crystals. The photoluminescence emission studies of grown crystals indicated the blue and green emission at 491 nm and 542nm, due to transition from the <sup>5</sup>D<sub>4</sub> excited state to <sup>7</sup>F<sub>6</sub> and <sup>7</sup>F<sub>5</sub> ground states respectively. The antibacterial activity studies showed that the grown crystals were more effective in killing pathogenic bacteria's which affect the human beings.

**Keywords:** Sulphamic acid, XRD, FTIR, EDAX, SEM.

---

### 1. Introduction

Bulk single crystals play a major role in modern technological devices because of their excellent physical and chemical properties. Therefore a vast majority of research activities have been concentrated on growth and characterization of pure and additive single crystals for identifying new applications in the modern world [1, 2]. Because of the high speed information processing, high optical data disk storage, frequency conversion, color display, ultra compact lasers, and optical communication, the inorganic crystals are used in the field of photonics [3,4]. Among all inorganic crystals, sulphamic acid has drawn great attention owing to its high stability, better transmittance and excellent optical and nonlinear properties [5,6].

Sulphamic acid (H<sub>2</sub>NSO<sub>3</sub>H, SA) and its derivatives possess high NLO property because of its two planar rings which originate from the strong donor-acceptor intermolecular interaction

and delocalized  $\pi$ -electron configuration [7]. Sulphamic acid is relatively stable and crystallizes in non-centrosymmetric structure which results in excellent NLO property. The sulphamic acid is a white crystalline, odorless, non-volatile, non-hygroscopic, inexpensive and non-corrosive solid. Also it acts as an efficient green catalyst in organic synthesis [8, 9]. Interestingly, sulphamic acid is a sulphur-containing amino acid with mild acidity and also exists as  $\text{H}_3\text{N}^+\text{SO}_3^-$  zwitter ionic units, which is immiscible with commonly employed non-polar organic solvents [10, 11]. Recent studies revealed that sulphamic acid can be used as a best substitute for conventional Bronsted and Lewis acid catalysts [9].

Due to high thermal stability, enhanced catalytic behavior and excellent optical properties numerous research activities have been done based on sulphamic acid with different dopants and additives. The previous studies revealed that various dopants like lanthanum, copper, manganese, nickel, dysprosium, terbium, thiourea, neodymium, Cesium, ferrous sulphate, urea, Gadolinium, Ammonium chloride, cerium, Lithium chloride, NaCl & KCl,  $\text{Mg}^{2+}$  &  $\text{Fe}^{2+}$ , NaCl, Yttrium,  $\text{ZnSO}_4$  &  $\text{MnSO}_4$ , Nitric acid have been added to sulphamic acid and their structural properties have been investigated. In the present work sulphamic acid and amino acid added sulphamic acid crystals were grown by slow evaporation method and its structural, mechanical and optical properties were investigated.

## **2. Experimental Methods**

The pure sulphamic acid and amino acid added sulphamic acid crystals were grown by slow evaporation method from the AR grade sulphamic acid and amino acid powders. Amino acid added sulphamic acid was grown by adding AR grade sulphamic acid and amino acid in the molar ratio 3:1 in deionized water. The mixture was stirred well using magnetic stirrer for four hours at room temperature to get the clear saturated solution. The well saturated solution was then filtered using a filter paper to remove any immiscible and unstirred chemicals and to get clear solution. The filtered solution was then transferred to crystal growth vessels, covered by aluminum foil sheet with some punched holes and kept in a dust free atmosphere. At room temperature the solution was allowed for crystallization. Good transparent and colorless crystals were harvested after 20 days. Fig 1 shows the photograph of the grown sulphamic acid (named as SA), glycine added sulphamic acid (named as GSA), L-isolucine added sulphamic acid (named as LISA) and L-Phenyl alanine added sulphamic acid (named as LPASA). Figure 1 shows the photographs of the grown crystals.

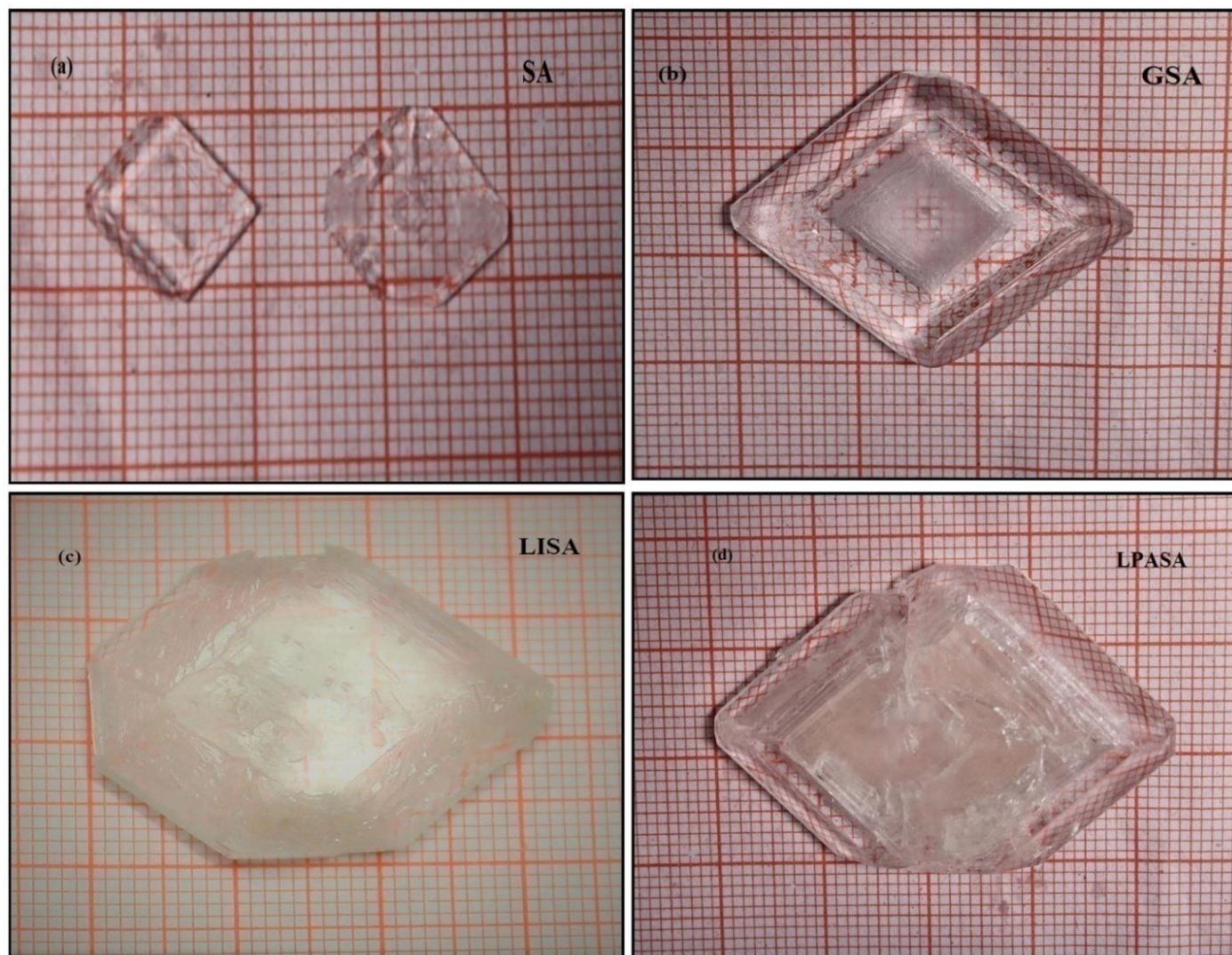


**Fig 1. Photographs of the grown (a) SA (b) GSA (c) LISA and (d) LPASA crystals.**

Powder X-ray diffraction (PXRD) analysis was carried out by irradiating the crystal with  $\text{Cu K}_\alpha$  radiation ( $\lambda = 1.5406\text{\AA}$ ) using PANalytical XPERT-PRO diffractometer. The sample is scanned for a  $2\theta$  range of  $10^\circ$ - $80^\circ$ . The Fourier transform infrared (FTIR) spectra was recorded between  $4000$  to  $400\text{cm}^{-1}$  by using Thermo Nicolet 380 FTIR spectrophotometer. Raman modes were examined using imaging spectrograph STR 530mm Focal Length Laser Raman Spectrometer. The surface morphology of grown crystal was investigated by using Scanning Electron Microscope of VEGA3TESCAN at 228x and 347x magnification. The EDAX spectrum was recorded by Bruker Nano GmbH Berl in, Germany Esprit 1.9. UV-VIS analysis of the grown crystal is carried using UV-DRS spectrophotometer in the wavelength range of 190-1100nm. The Vickers hardness of the samples was measured using the Shimadzu Model-HMV-2T. Thermo gravimetry (TG) and differential thermal analysis (DTA) were measured at a heating rate  $20^\circ\text{C}/\text{min}$  between  $35^\circ\text{C}$  and  $1000^\circ\text{C}$  in  $\text{N}_2$  atmosphere using Exstar/6300. The photoluminescence of the grown crystals were studied using Varian Cary Eclipse photo

luminescence spectrophotometer. The antibacterial activity of the grown crystals was studied by Disk Diffusion Method and Kirby – Bauer methods

### 3. Results and discussions

#### 3.1. Powder X-ray diffraction

The powder x-ray diffraction (PXRD) pattern of sulphamic acid and amino acids added sulphamic acid were shown in Fig 2. All the diffraction peaks were well matched with the standard ICDD pattern (JCPDS Card No.: 70-0060). No unindexed peaks have been identified. The strong intensity peak (221) was obtained for pure sulphamic acid (Fig 2a). Therefore most of the grains were oriented in the [221] direction. The intense peaks (021), (210) and (211) belonged to orthorhombic structure was also identified. Hence the synthesized crystals were phase pure and possessed orthorhombic structure [12]. Upon addition of glycine, L-isolucine and L-phenyl alanine with sulphamic acid the crystal structure was not changed. Only intensity modification was observed. In GSA, LISA and LPASA samples the most intense peak was (211) similar to pure sulphamic acid. Further the intensity of (221), (102), (021) and (210) were reduced drastically. Therefore the preferred grain orientation was along [211] plane. However, no impurity peaks were noticed. All the peaks were well fitted to the orthorhombic crystal structure [13]. Hence the same crystal system was maintained on addition of amino acids.

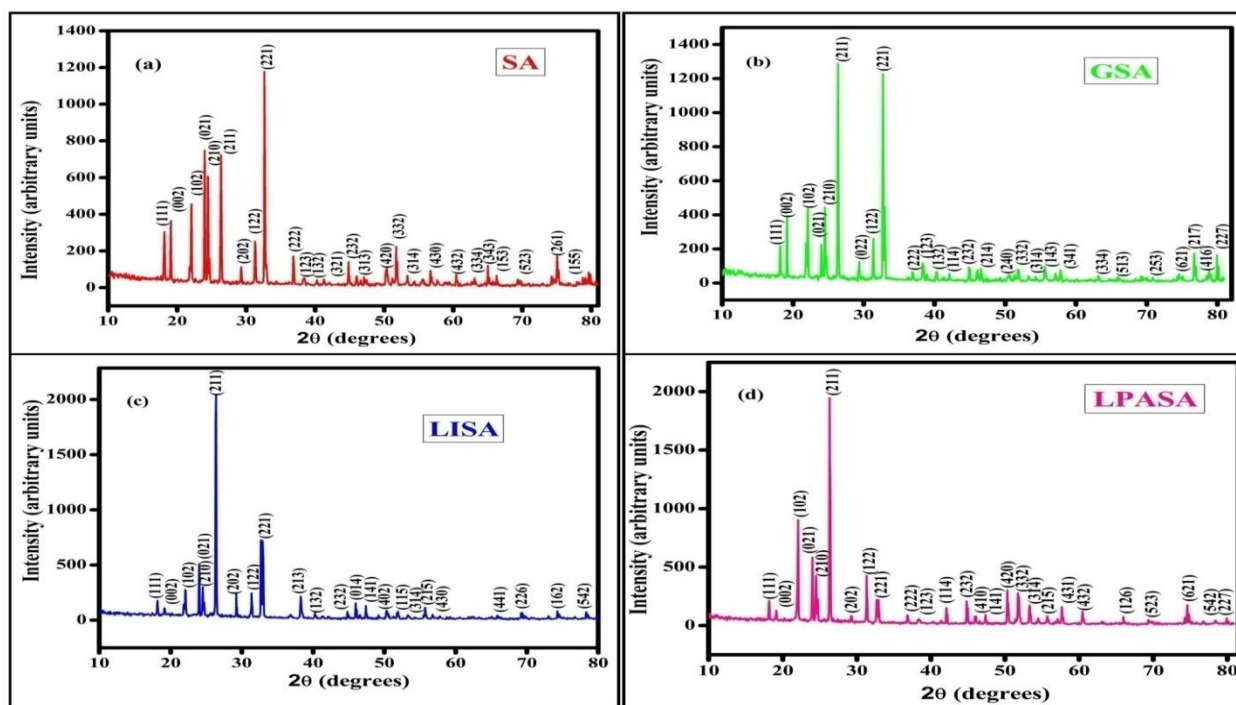


**Fig 2.** Powder X-ray diffraction patterns of (a) SA (b) GSA (c) LISA and (d) LPASA crystal

Using unit cell software package the unit cell parameters were calculated and tabulated. From the Table 1, it was found that cell parameters were in good fit to standard lattice parameters of sulphamic acid. Addition of glycine to sulphamic acid resulted in elongation along the c-axis of the orthorhombic cell, whereas meager variation was seen in b-axis. But due to elongation of c-axis, the volume of the lattice has been increased. Addition of L-isolucine to sulphamic acid lead to elongation of the a-axis and shrinkage of b and c axis of the orthorhombic cell. Therefore, the volume of the lattice has been decreased due to shrunken unit cell. This also confirmed the addition of L-isolucine in to the lattices of SA. Addition of L-phenyl alanine reduces the unit cell volume even though there was elongation in b and c-axis. The reduced cell volume was due to the contraction along a-axis.

Comparing to amino acid added sulphamic acid to pure SA the unit cell parameters as well as cell volume were varied. This indicated that the added amino acids were incorporated into the lattice of SA. In GSA a-axis almost remained the same whereas the b and c-axis were elongated which lead to increase in cell volume. Moreover in LISA and LPASA added SA all the axis parameters were reduced than pure SA but a hike was noticed in LISA added SA in a-axis. But the cell volume was decreased. The reduction of cell volume and cell parameters may be due to change in the orientation of the structure.

**Table 1. Structure and lattice parameters of pure SA, GSA, LISA and LPASA crystals.**

Crystal	Structure	a(A°)	b(A°)	c(A°)	Volume(A <sup>3</sup> )
SA	Orthorhombic	8.1266	8.0928	9.2298	607.0166
GSA	Orthorhombic	8.1262	8.0944	9.2408	607.8366
LISA	Orthorhombic	8.1573	8.0788	9.1324	601.8355
LPASA	Orthorhombic	7.9649	8.1087	9.2860	599.7360

### **3.2. Fourier Transform Infrared Analysis**

The recorded FTIR spectra of pure SA and amino acid added SA crystals are presented in Fig 3. The FTIR spectrum of SA and amino acid added SA showed the characteristic bonding of all the functional groups. The functional groups were assigned and summarized in Table 2. The IR band appeared at  $1002\text{ cm}^{-1}$  was related to the rocking mode vibration of  $\text{NH}_3^+$  ion thus confirmed the zwitter ionic nature of sulphamic acid crystal. The bands observed at frequencies around  $2873\text{ cm}^{-1}$  and  $3153\text{ cm}^{-1}$  respectively was due to  $\text{NH}_3^+$  vibrations correlated to symmetric as well as degenerative stretching modes. Moreover, the bands noticed at  $1447\text{ cm}^{-1}$ ,  $1806\text{ cm}^{-1}$  and  $1541\text{ cm}^{-1}$  successively were affirmed to symmetric and degenerated modes of vibration related to  $\text{NH}_3^+$  deformation. The vibration bands observed at  $1267\text{ cm}^{-1}$  and  $1068\text{ cm}^{-1}$  were relatively due to degenerated and symmetric  $\text{SO}_3^-$  stretching modes [13]. The band occurred at  $548\text{ cm}^{-1}$  was also assigned to degenerated  $\text{SO}_3^-$  deformation. The N-S, N-H and S-H stretching vibrations were seen at frequencies  $690\text{ cm}^{-1}$ ,  $2023\text{ cm}^{-1}$  and  $2458\text{ cm}^{-1}$  respectively [14]. All the observed IR bands are in good agreement the recorded FTIR spectrum of sulphamic acid. All the characteristic IR bands of functional groups as well as zwitter ions were observed in the synthesized SA crystal were in accordance to previous reports [5, 15]. Hence it was evident that the synthesized SA crystal was phase pure and exhibited orthorhombic structure. However in glycine added sulphamic acid the band intensities were decreased drastically. Only weak peaks were seen and some peaks related to  $\text{NH}_3^+$  vibrations have been disappeared. In L-isolucine added sulphamic acid all the peaks were seen whereas the band intensities were changed. In L-phenyl alanine added crystals almost all the modes were appeared. But the intensities were drastically decreased which revealed that there may be subtle change in the geometry of the sub lattice. In both LISA and LPASA crystals the changes occurred were more or less same, whereas the peak intensities were varied. These changes indicated that they have same chirality. But in GSA crystals drastic change was seen which may be due to the change in geometry of the lattice.

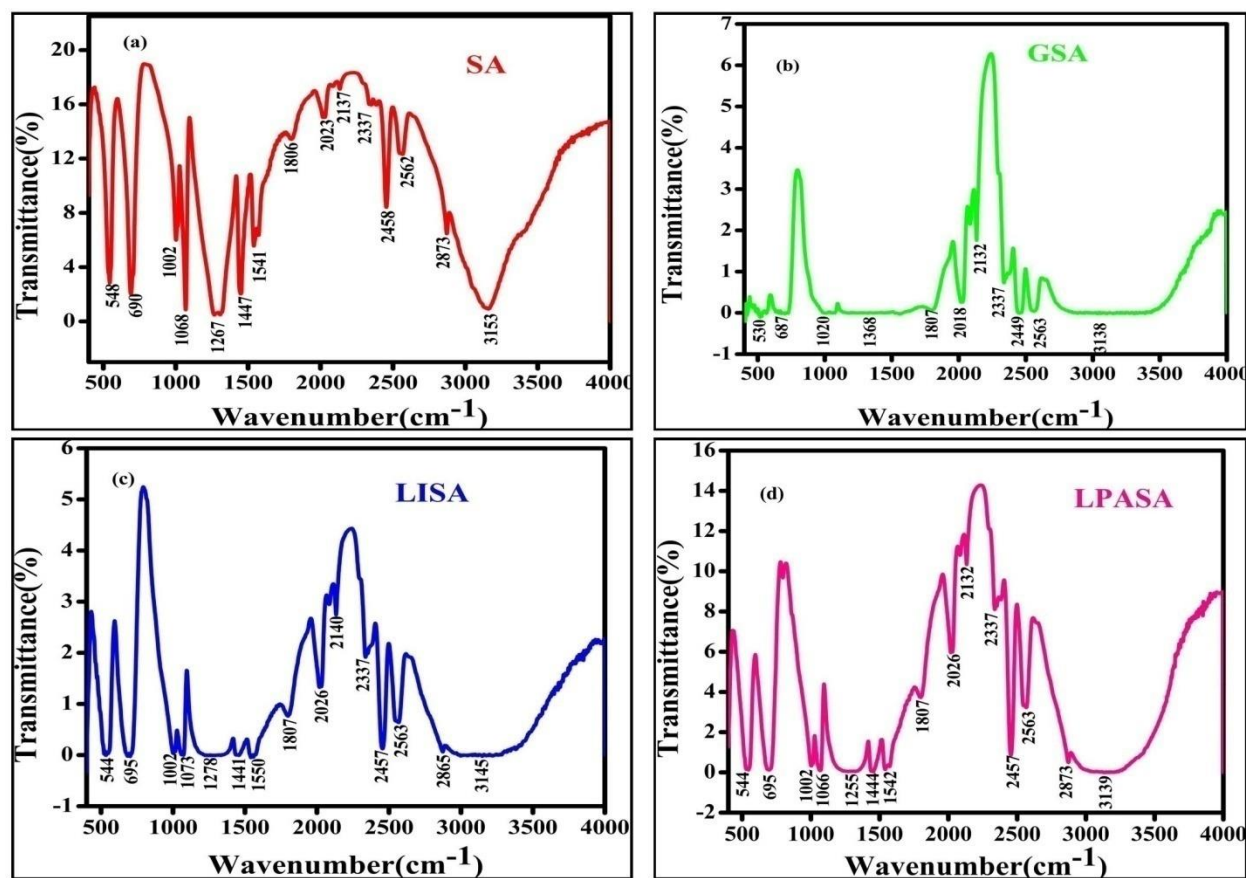


Fig 3. FTIR spectra of (a) pure SA (b)GSA (c) LISA and (d) LPASA crystal

Table 2. Vibrational assignment of the pure and amino acids added SA crystal

Wave number( $\text{cm}^{-1}$ )				Assignment
SA	GSA	LISA	LPASA	
548	530	544	544	Degen. $\text{SO}_3^-$ deformation
690	691	695	695	N-S stretching
1002	1002	1002	1002	Rocking mode $\text{NH}_3^+$
1068	-	1073	1066	Symmetric $\text{SO}_3^-$ Stretching
1267	-	1278	1272	Degen. $\text{SO}_3^-$ stretching
1447	-	1441	1444	Sym. $\text{NH}_3^+$ deformation
1541	-	1550	1542	Degen. $\text{NH}_3^+$ deformation

1806	1807	1807	1807	Symmetric $\text{NH}_3^+$ deformation
2023	2018	2026	2026	N-H Stretching
2458	2449	2457	2457	S-H Stretching
2873	-	2865	2873	Symmetric $\text{NH}_3^+$ Stretching
3153	3138	3145	3139	Degen. $\text{NH}_3^+$ Stretching

### 3.3 Raman analysis

The Raman spectra of SA and amino acids added SA crystals are shown in Fig 4. The high intensity vibration band occurred in the frequency region near  $1059\text{cm}^{-1}$  was due to symmetric  $\text{SO}_3^-$  stretching vibration. The vibrations appeared at  $1281\text{cm}^{-1}$  and  $1345\text{cm}^{-1}$  were related to degenerated  $\text{SO}_3^-$  stretching modes. The band seen at  $1017\text{cm}^{-1}$  was assigned to degenerated  $\text{NH}_3^+$  rocking vibration. The N-S stretching vibration was observed at  $682\text{cm}^{-1}$  [16]. The vibration bands observed at  $543\text{cm}^{-1}$  was assigned to degenerated  $\text{SO}_3^-$  deformation and vibration band observed at  $363\text{cm}^{-1}$  was due to the presence of  $\text{SO}_3^-$  rocking vibrations. The vibration bands noticed at  $256\text{cm}^{-1}$  was assigned to N-S torsion [17-20]. All the Raman modes attributed to the orthorhombic structure of SA crystal was displayed in the Raman spectra. Hence the structure of SA crystal was confirmed. In glycine added sulphamic acid major changes in vibration bands were not observed. Only slight shift in peak positions were noticed and the intensity of the peaks were increased. The main observation from the Raman spectra was the intensity of the high intense vibration band associated to symmetric  $\text{SO}_3^-$  stretching was improved and was moved to higher wave number. All the other peaks were almost remained in the same peak positions. Therefore it was confirmed that the addition of glycine to sulphamic acid never disturbed the structure of sulphamic acid, however subtle changes have been happened in the geometry of the structure. Hence it was confirmed that the orthorhombic crystal system was still retained in the synthesized glycine added crystals. In L-Isolucine added sulphamic acid only slight changes in peak positions were observed. The intensity of the high intense vibration band associated to degenerated  $\text{SO}_3^-$  deformation was almost retained in the same peak position. All the other peaks were slightly deviated than pure SA. Therefore it was elucidated that the addition of L-Isolucine to sulphamic acid not ever disturbed the structure of sulphamic acid, anyway small variations have been occurred in the geometry of the structure. In L-phenyl alanine added crystals only shift towards higher wave number was noticed. Also it was found that the intensity of the  $1059\text{cm}^{-1}$  peak related to symmetric  $\text{SO}_3^-$  stretching vibration was increased on addition of amino acids which confirmed the change in the geometry of the lattice even though the same orthorhombic structure was retained.



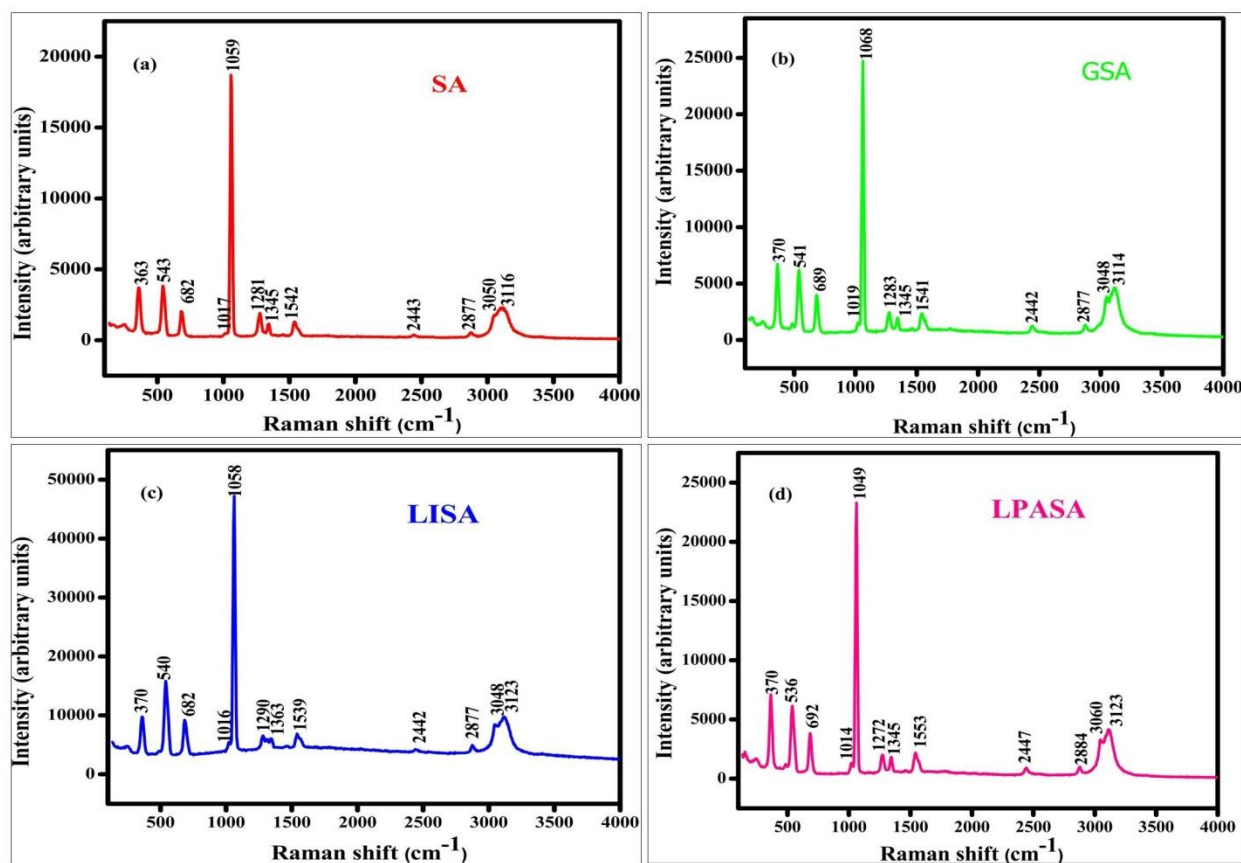


**Fig 4. Raman spectra of (a)SA (b)GSA (c) LISA and (d) LPASA crystal**

### 3.4 Morphology and compositional analysis

SEM micrographs of SA and amino acids added SA crystals are shown in Fig 5a. From the micrographs it was found that the grains were non uniform in size and shape. Non-uniformity in shape and size may be due to uneven distribution of temperature during the growth process [4]. On close examination of the micrographs it was noticed that that crystals were agglomerated as clusters and voids were seen.

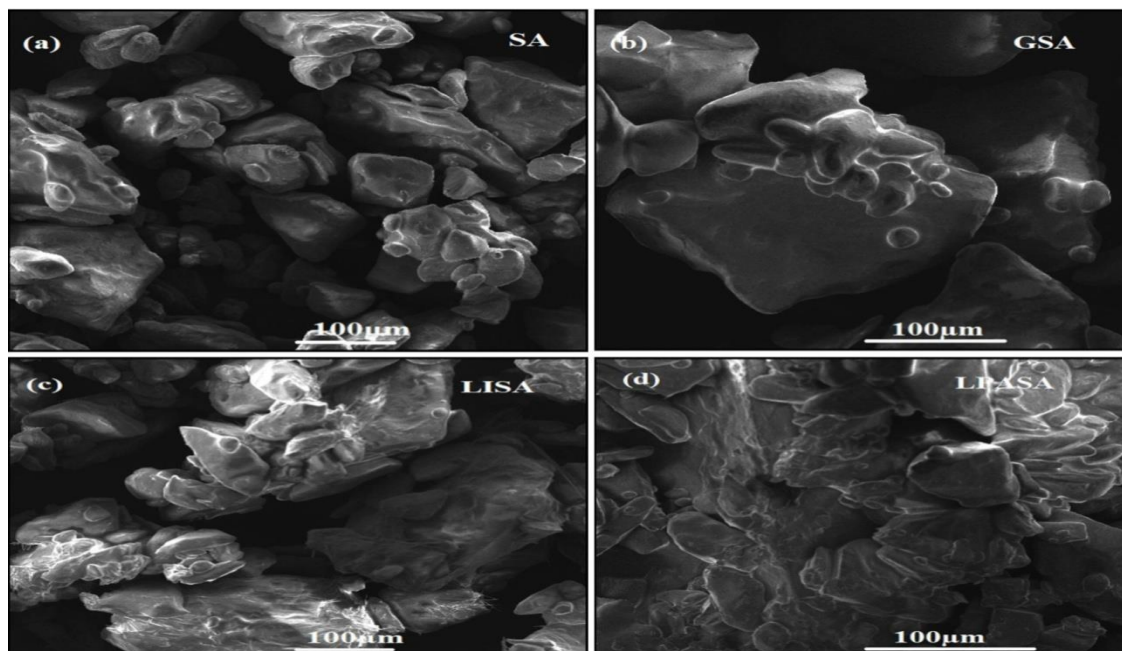


**Fig 5a. SEM analysis of (a)SA (b)GSA (c) LISA and (d) LPASA crystal**

The EDAX spectra of SA and amino acids added SA crystals are shown in Fig 5b. The spectra showed the presence of constituent elements sulphur (S), nitrogen (N) as well as oxygen (O) respectively. Also the peak linked to carbon was noticed along with other elements. This confirmed the incorporation of carbon into the lattice. The elemental compositions were represented in Table 3a, 3b, 3c & 3d.

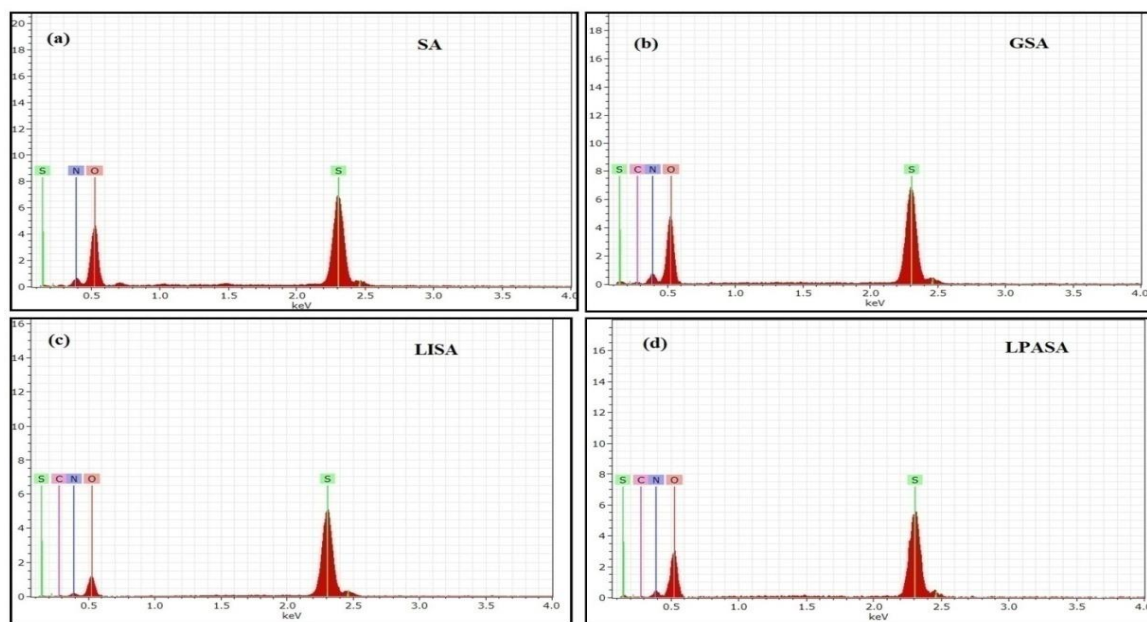


**Fig 5b. EDAX analysis of (a) SA (b) GSA (c) LISA and (d) LPASA crystal**

**Table 3a. Elemental composition of pure SA**

Element	Atomic weight (%)	Molecular weight (%)
Sulphur	12.37	22.51
Oxygen	69.71	63.26
Nitrogen	17.91	14.23

**Table 3b. Elemental composition of GSA**

Element	Atomic weight (%)	Molecular weight (%)
Sulphur	10.53	19.75
Oxygen	64.77	60.65
Nitrogen	19.16	15.70
Carbon	5.54	3.90

**Table 3c. Elemental composition of LISA**

Element	Atomic weight (%)	Molecular weight (%)
Sulphur	19.95	34.61
Oxygen	52.48	45.42
Nitrogen	19.08	14.45
Carbon	8.48	5.51

**Table 3d. Elemental composition of LPASA**

Element	Atomic weight (%)	Molecular weight (%)
Sulphur	13.58	24.56
Oxygen	65.87	59.47
Nitrogen	18.05	14.27
Carbon	2.50	1.69

### 3.5. UV-VIS studies

UV-VIS analysis of the grown crystals recorded in the wavelength range 200nm to 800nm is shown in Fig 6. The transmission graph showed that both SA and amino acids added crystal has wide range of transparency window approximately above 360 nm. The transmission of SA and amino acids added crystal was found to be 86%, 91%, 91% and 92% respectively. Enlargement of transmission was observed for amino acids addition in sulphamic acid. High transmittance has been noticed in the entire visible region and hence verified that the crystals possessed good quality [21]. The absorption spectrum of SA and amino acids added crystal crystals are shown in Fig 7. The figure showed the lower cut-off wavelength for SA crystal was at 226 nm whereas for amino acids added crystal it was around 230 nm, 228nm and 234nm respectively. To calculate

the energy band gap values, the Tauc's plot was drawn and was shown in Fig 8. From the plot the optical band gap for SA and amino acids added SA crystals were evaluated and the values were found to be 3.7eV, 3.3 eV, 3.2eV and 3.0eV respectively. Here it was found that the band gap was reduced upon addition of amino acids.

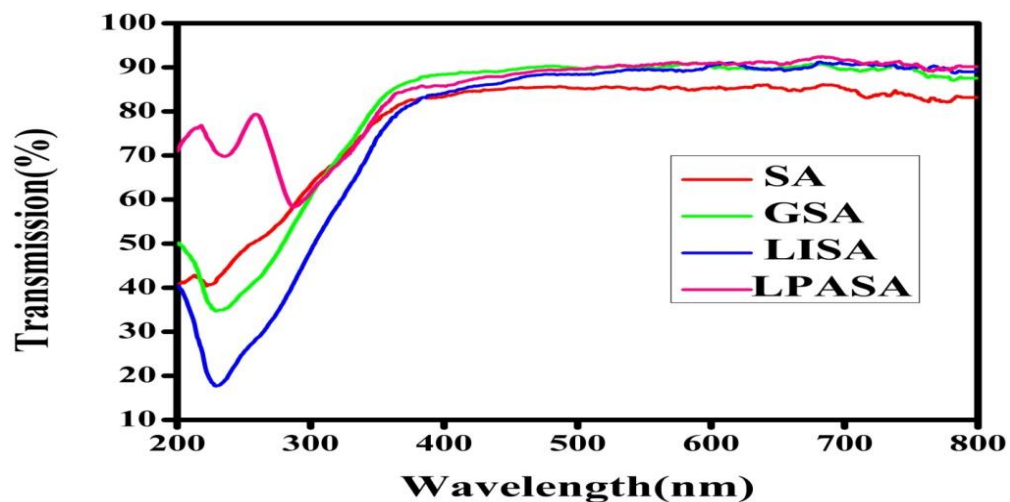


Fig 6. UV Transmission spectra of pure and amino acids added SA crystal.

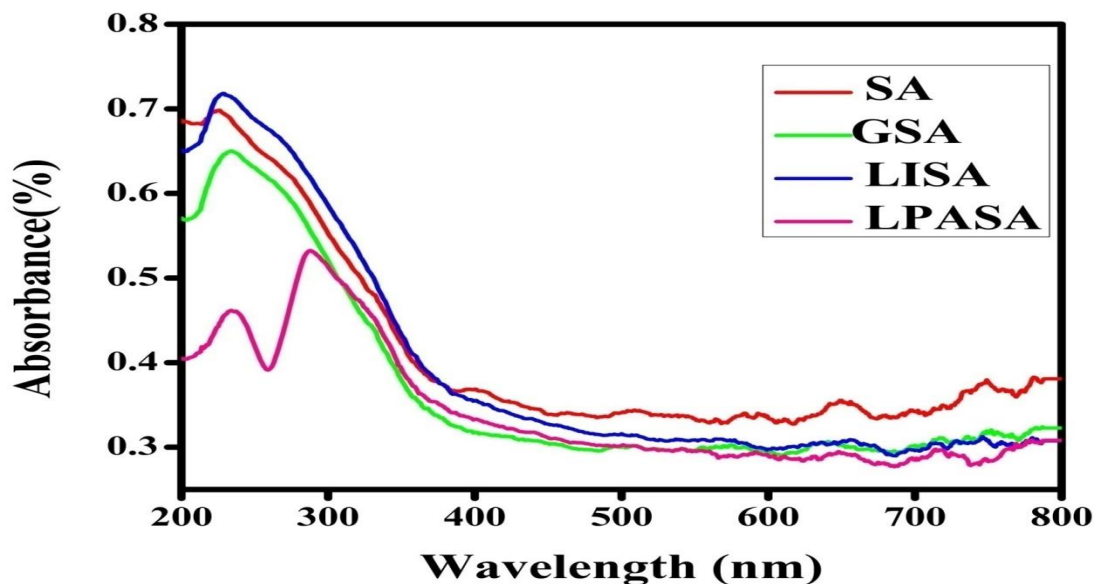
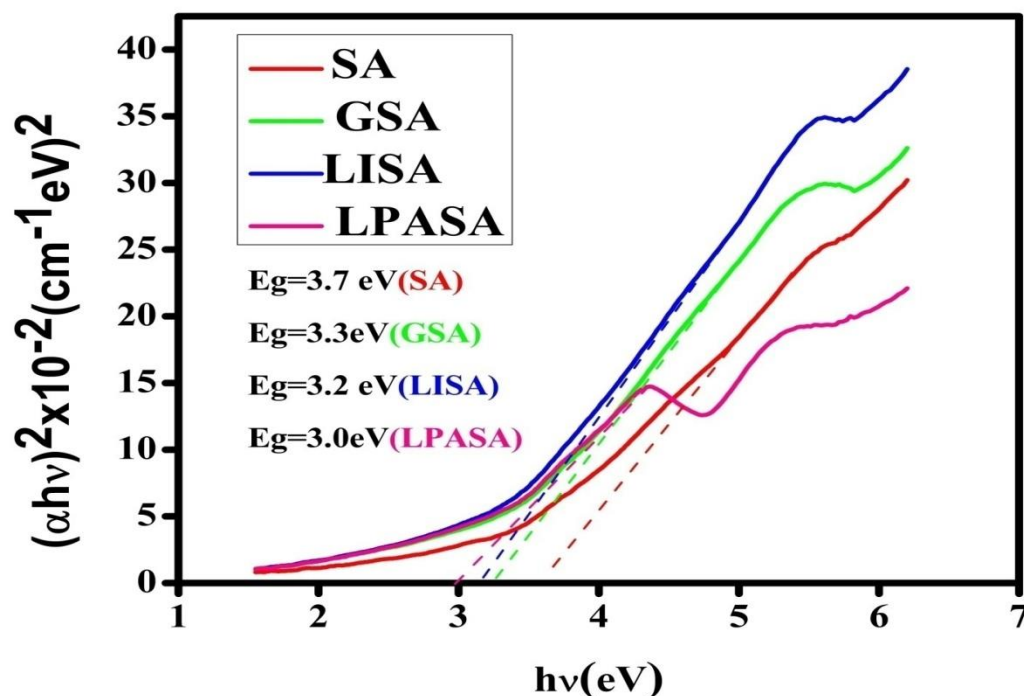


Fig 7. UV Absorption spectra of pure and amino acids added SA crystal.



**Fig 8.**Tauc's plot for pure and amino acids added SA crystal

### 3.6. Vickers's Hardness Test:

Hardness of a material is usually calculated as a measure of the resistance it offers to local deformation. To determine the mechanical behavior of the materials, hardness measurement was done. In order to measure the hardness, different loads of magnitudes varying from 25gm to 100gm was applied for a fixed interval of time over a well-polished grown crystal and the Vickers micro hardness number ( $H_v$ ) was calculated using the formula  $H_v = 1.8544P/d^2 \text{kgmm}^{-2}$  where  $P$  is the applied load (kg) and  $d$  is the average diagonal length of indentation (mm). A graph between Hardness number ( $H_v$ ) and applied load ( $P$ ) is shown in Fig 9. From the graph it was found that the hardness of the crystal was increased with increase in load. Up to 100 g no cracks have been noticed. Also the hardness of SA was increased upon amino acids addition which demonstrated that the addition of amino acids improve the hardness of SA [4]. Similar behavior has been reported for metal ion doped SA crystals [13]. According to Onitsch and Hannemann, a crystal can be defined as hard or soft based on the hardening coefficient. The plot between  $\log p$  versus  $\log d$  gives the hardening coefficient. If the coefficient lies between 1 and 1.6 then they are listed under hard materials and for soft materials it is above 1.6 [4, 22]. Fig 10 shows the graph of  $\log p$  versus  $\log d$ . The slope of both SA and amino acids added SA

was above 1.6 and so they were considered as soft crystals.

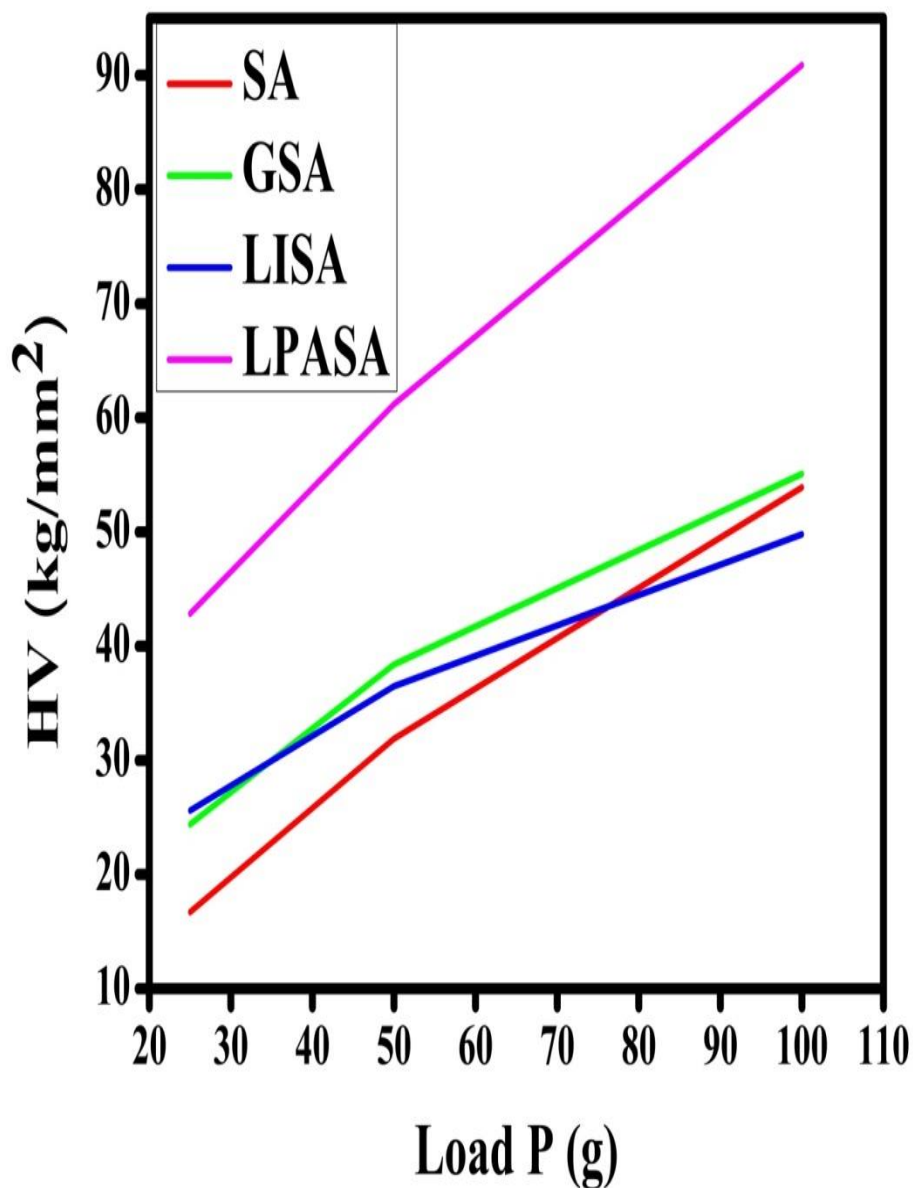


**Fig 9 Plot of Load (P) Vs Hardness number (Hv) for pure and amino acids added SA crystal.**

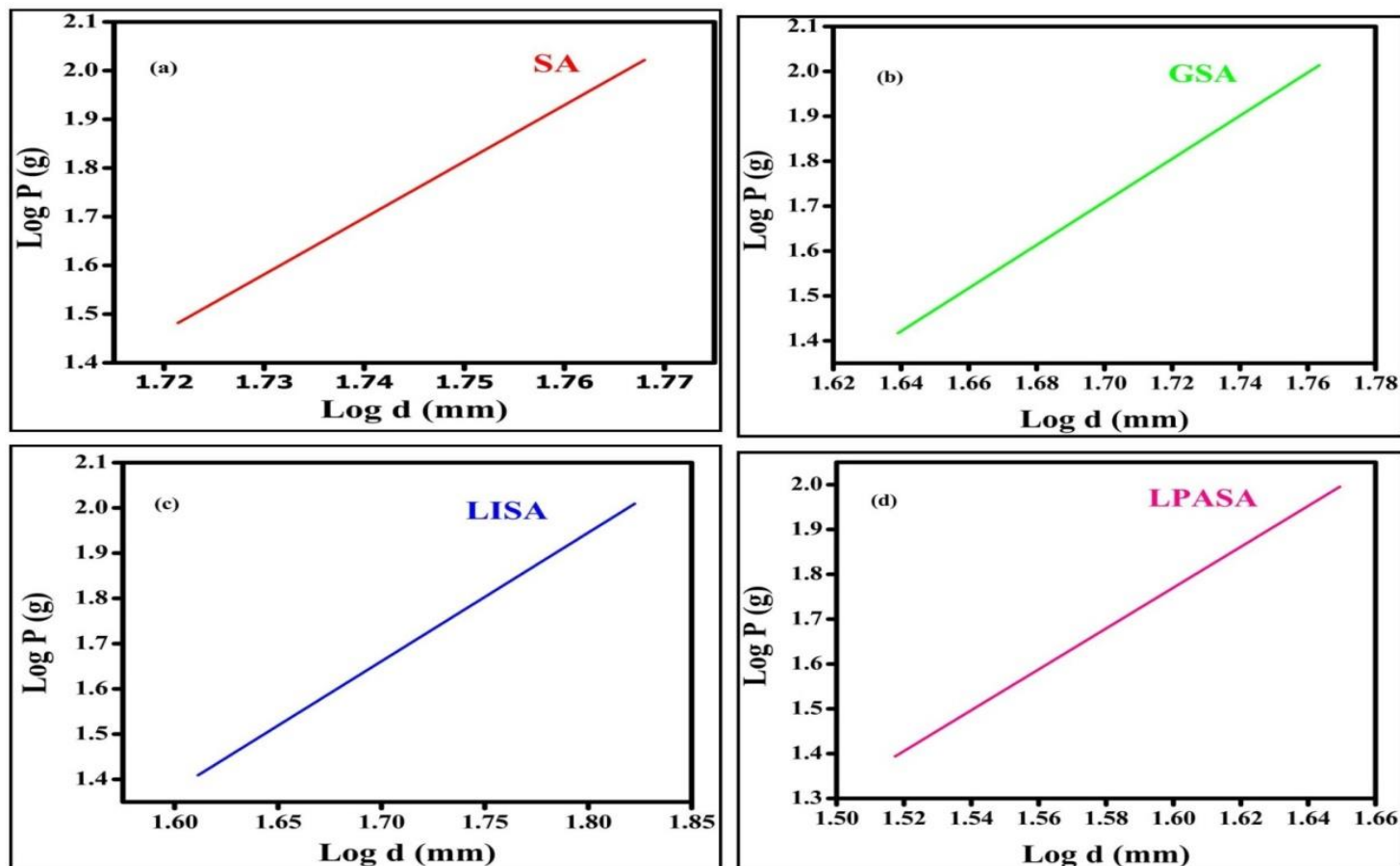


Fig 10. Log p Vs Log d for (a) SA (b) GSA (c) LISA and (d) LPASA crystal

### 3.7. TG-DTA Analysis

The observed TG-DTA curves of SA and amino acids added SA samples are shown in Fig 11. From the graph it was clear that no weight loss occurred up to 261 °C for SA crystal. An abrupt loss in weight has been occurred from 261 to 448 °C and sharp steep peak was observed at 448 °C for SA crystal which confirmed the decomposing nature of the crystal at that temperature as reported by Brahmaji et al [4]. In DTA curve, endothermic peaks were seen at 212 °C and 261 °C which correspond to the evaporation of water and solvent molecules completely. Further increase of temperature led to weight loss of the material and related to decomposition temperature of the crystal due to the occurrence of sharp endothermic peak at 448 °C for SA crystal similar to previous studies [6]. Similar changes have been observed in amino acids added SA crystals, but the temperatures have been shifted to the higher end in GSA and LPASA crystals. This predicts that glycine and L-phenyl alanine added sulphamic acid attained more stability than pure sulphamic acid. Hence the synthesized crystals possessed good thermal stability approximately up to 275 °C and suitable for applications under this temperature

range, and slightly lowered temperature for LISA crystal probably at 205°C and 257°C respectively which were related to loss of water molecules and solvent elements.

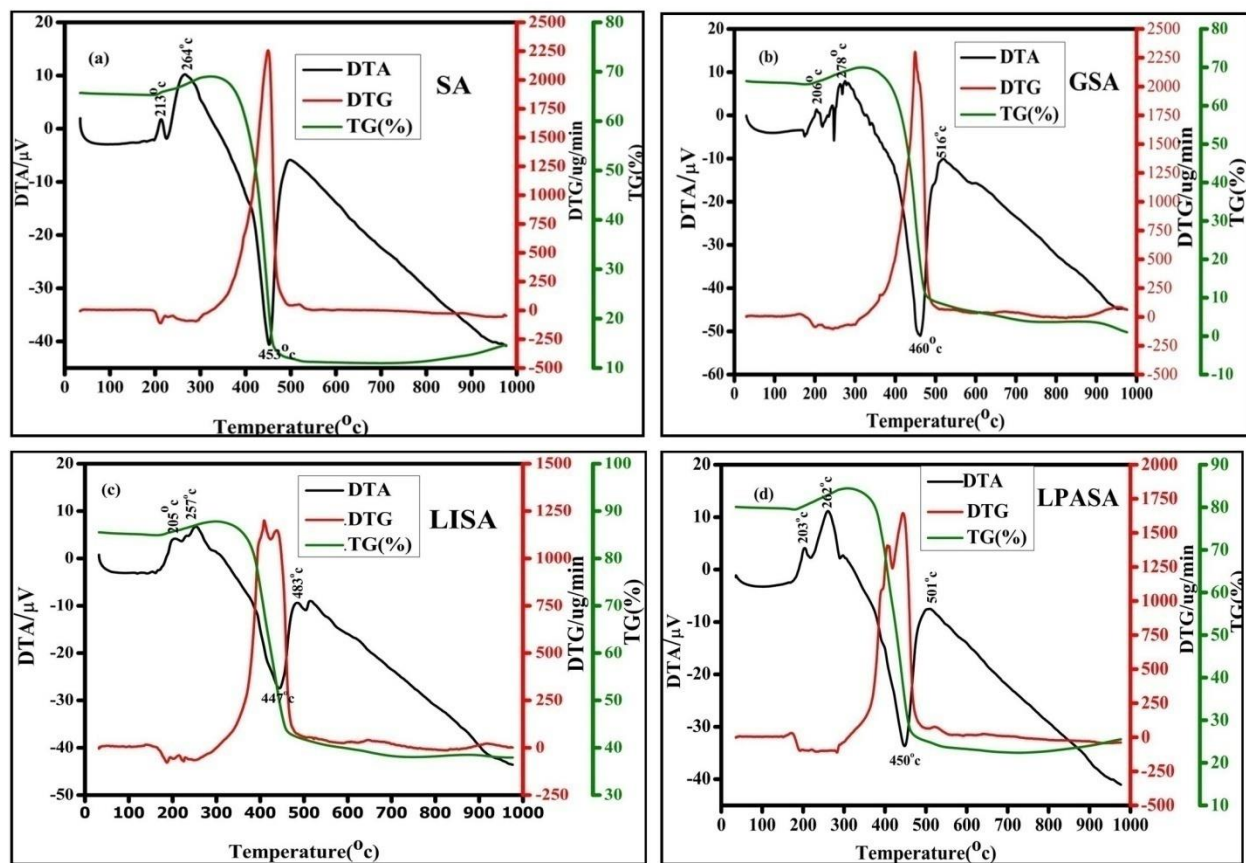


Fig 11. TG-DTA curves of (a) SA (b) GSA (c) LISA and (d) LPASA crystal

### 3.8 Photoluminescence studies:

Fig. 12 displays the emission spectra of SA and amino acids added SA crystals. The emission spectra showed emission in the ultraviolet and visible regions. In the visible region violet, blue and green emissions were observed. The strongest emission was occurred at 490 nm related to blue emission. The peaks observed below 400 nm observed in the ultra violet region were due to electronic transition  $\pi\pi^+$  as reported by Arumugam et al [23]. The peaks observed below 500 nm were related to blue emission [24]. Due to transition between the energy levels  $^5D_4$  to  $^7F_6$ , these emissions were occurred. The peak noticed at 530 was correlated to green emission due to transition from  $^5D_4$  to  $^7F_5$  energy levels [4]. The property of having strong emission in this range may prime to potential application of this material in optoelectronic devices [25].



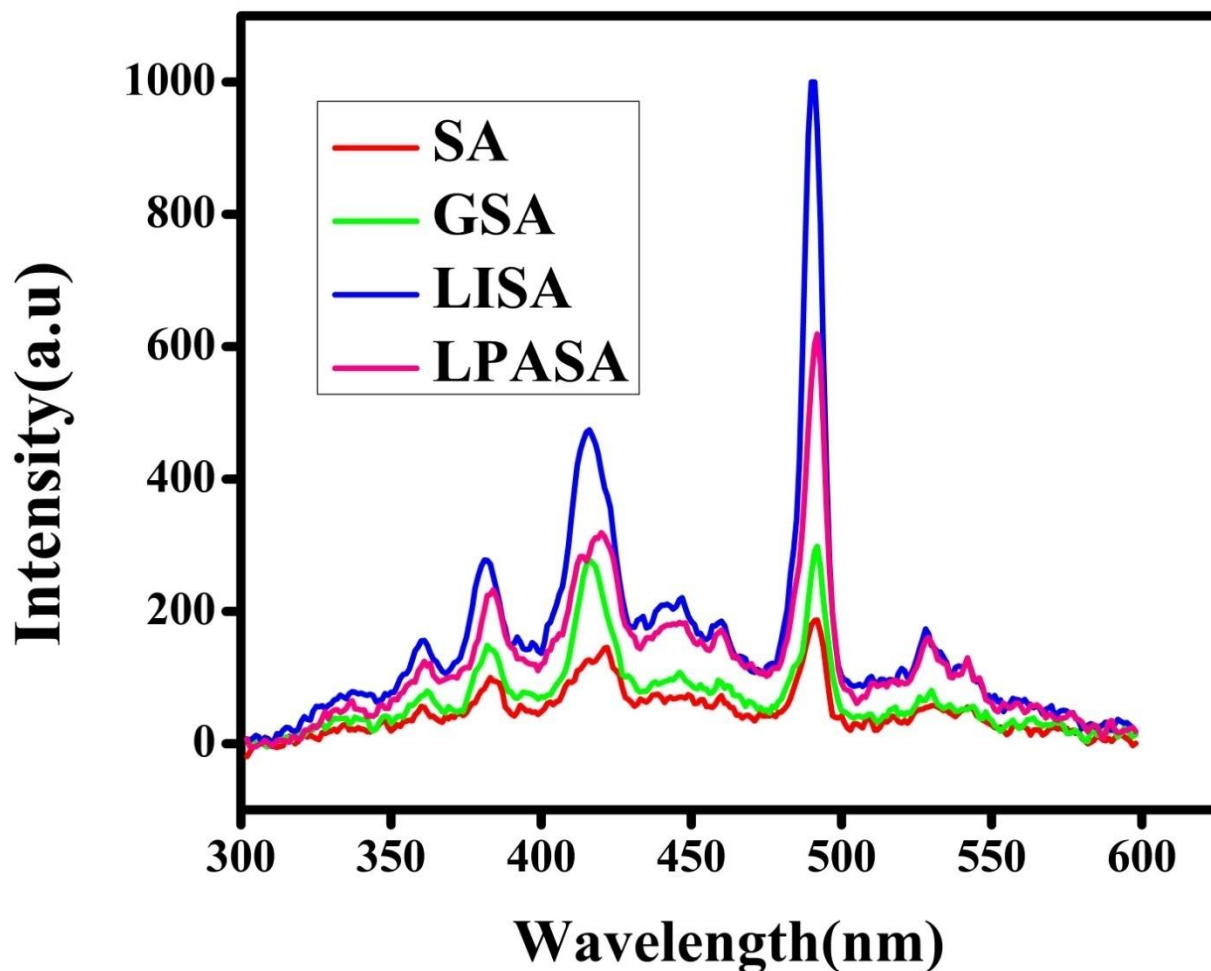


Fig 12. Photoluminescence spectra of pure SA and amino acids added SA crystal.

### 3.9 Antibacterial activity:

The antibacterial activity of SA and aminoacids added SA was investigated against gram positive bacteria (*Bacillus*, *staphylococcus aureus*) and gram negative bacteria (*Escherichia coli*, *klbsiela*, *serattia*) by Disk Diffusion method and Kirby – Bauer method. Reagents used for the Disk Diffusion Test are Mueller-Hinton Agar medium.

For known standard antibiotic, the zone of inhibition for *E.coli* has 22mm of half lifes. The present study revealed that for the pure and amino acid added SA, the zone of inhibition is high. Among all, for LISA the zone of inhibition was increased upto 36. This observation confirms that LISA sample has high power in killing bacterias. Similarly in *klebsiella*, *bacillus*, *staphylococcus aureus* and *serattia*, the absorbed zone of inhibition was increased when compared with standard antibiotic zone of inhibition. Table4 shows the

antibacterial activity of SA and amino acids added SA. From this we concluded that the grown crystals are more effective than standard antibiotic inhibition. Hence it was found that the grown crystals can be used in detergents for killing bacterias [26].

**Table 4. Antibacterial effect of pure SA and aminoacids added SA crystal.**

Bacteria name	SA Zone of inhibition[mm]	GSA Zone of inhibition[mm]	LISA Zone of inhibition[mm]	LPASA Zone of inhibition[mm]	Standard antibiotic AMIKACIN Zone of inhibition[ mm ]
E.COLI	28	32	36	29	22
KLEBSIELLA	30	31	34	31	19
BACILLUS	29	33	34	30	20
STAPHYLOCOCCUS AUREUS	26	31	34	27	22
SERATTIA	33	33	31	33	19

#### 4. Conclusion

SA and amino acids added SA single crystals were grown successfully by slow evaporation method at room temperature. Powder X-ray diffraction studies confirmed the crystalline nature and orthorhombic structure of the synthesized crystals. FTIR and FT-RAMAN analysis revealed the stretching and deformation vibrational modes of  $\text{NH}_3^+$  and  $\text{SO}_3^-$ . The morphological and compositional analysis proved that, on addition of amino acids in SA, the crystallinity was improved and the presence of carbon was identified. The optical study showed that the crystalline perfection was excellent and the transparency was enhanced upon addition of aminoacids. The value of band gap was found to decrease with the addition of amino acids in SA. Vicker's micro hardness studies proved that the grown crystals belonged to soft material and the hardness of the material was increased with load. Thermal stability was confirmed by thermal analysis and found that the synthesized SA and amino acids added SA crystals are thermally

stable up to 261°C, 278°C, 257°C and 258°C respectively. The photoluminescence studies showed the SA and amino acids added SA crystals emitted UV and visible radiations. The most prominent emission was in the blue region due to transition from  $^5D_4$  to  $^7F_6$  energy levels. Since these crystals may find application in optoelectronic devices. The antibacterial activity showed that upon addition of amino acid the antibacterial activity was enhanced. But L-isolucine added sulphamic acid (LISA) showed a higher antibacterial activity than other amino acids which will be helpful for killing pathogenic bacterias.

## **5. References**

- [1] Sangwal K, Prog. Cryst. Growth Charact. Mater 32(1996) 3.
- [2] Veintemillas-Verdaguer S, Prog. Cryst. Growth Charact. Mater 32(1996) 75.
- [3] Samson Yesuvadiana, Anbarasu Selvaraj, Martina Mejeba Xavier Methodius, Bhagavannarayana Godavarti, Vijayan Narayanasamy and Prem Anand Devarajan, Optik 126 (2015) 95.
- [4] Brahmaji B, Rajyalakshmi S, Visweswara Rao T K, Srinivasa Rao Valluru, EsubBasha S K, Satyakamal Ch, Veeraiah V and Ramachandra Rao K, Journal of science: Advanced Materials and devices 3 (2018)68.
- [5] Jaishree D, Kanchana G and Kesavasamy R 2014 Adv. Condens. Matter phys. 2014 1
- [6] Brahmaji B, Rajyalakshmi S, Satyakamal Ch, Veeraiah V, Ramachandra Rao K, Veerendra atla and Venkateswara Rao K, 2017 Optical Materials 64 100
- [7] Rafi Ahamed S and Srinivasan 2012 Elixir Crystal Growth 50 10628
- [8] Bo Wang Synlett 8 (2005) 1342.
- [9] Wang Bo, Ming Y L and Shuan S J 2003 Tetrahedron Lett. 44 5037
- [10] Marcelo G, Montes D'Oca, Rafael Marinho Soares, Renata Rodrigues de Moura and Vinicius de Freitas Granjao, 2012 Fuel 97 884.
- [11] Canagaratna M, Philips J A, Goodfriend H and Leopold K R 1996 J. Am. Chem. Soc. 118 5290
- [12] Shakir M, Riscob B, Ganesh V, Vijayan N, Gupta R, Plaza J, Dieguez E and Bhagavannarayana G, J. Cryst. Growth 380(2013) 228.
- [13] Ramesh Babu R, Ramesh R, Gopalkrishnan R, Ramamurthi K, and Bhagavanarayana G 2010 Spectrochim. Acta part A Mol. Biomol. Spectrosc. 76 470
- [14] Valluvan R, Selvaraju K and Kumararaman S 2006 Mater.Chem.Phys. 97 81
- [15] Haupa K, Bil A and Mielke Z 2015 J.phys.Chem. A 119 10724
- [16] Muthusubramanian P and Raj A S 1982 J. Mol. Struct 84 25
- [17] Lenin M, Balamurugan N and Ramasamy P 2007 Cryst. Res. Technol. 42 39
- [18] Philip D, Eapen A and Aruldas G 1995 J. Solid State Chem. 116 217
- [19] Vuagnat A M and Wagner E 1957 J. Chem. Phys. 26 77
- [20] Qian Li, Shourui Li, Kai Wang, Xiaodong Li, Jing Liu, Bingbing Liu, Guangtian Zou and Bo Zou 2013 J. Chem. Phys. 138 214505.
- [21] Rajesh P and Ramasamy P 2009 Materials Letters 63 2260

- [22] Esthaku Peter M and Ramasamy P 2016 Adv. Mater. Lett. 7 83
- [23] Arumugam J, Suresh N, Selvapandiyan M, Sudhakar S and Prasath M 2019 Heliyon 5 1
- [24] Sonia, Vijayan N, Medha Bhushan, Kanika Thukral, Rishabh Raj, Manurya K.K, Haranath D and Martin Britto Dhas S A 2017 J. Appl.Cryst. 50 763
- [25] Mansour N, Momeni A, Karimzadeh R and Amini M 2012 Optical materials express 2 740
- [26] Ambrose A M, 1943 J. Ind. Hyg. Toxicol. 25 26